ELSEVIER

Materials Science and Engineering A 485 (2008) 428–438

MATERIALS SCIENCE & ENGINEERING A

www.elsevier.com/locate/msea

Microstructures and mechanical properties of modified AZ31–Zr–Sc alloys

S.C. Wang [a,*], C.P. Chou [a], Y.C. Fann [b]

[a] *Department of Mechanical Engineering, National Chiao Tung University, Hsinchu 300, Taiwan, ROC*
[b] *Industrial Technology Research Institute, Jhudung 310, Taiwan*

Received 29 September 2006; received in revised form 2 August 2007; accepted 2 August 2007

Abstract

The effects of minor Zr and Sc on the microstructures and mechanical properties of AZ31 have been determined. It is well known that the ductility of AZ31 is strongly dominated by the grain size of the microstructure. The AZ31–Zr–Sc alloy is a new frontier for development of fine-grain magnesium alloys. This paper investigated the enhancement of the grain refinement and ductility of AZ31–Zr–Sc alloys. A series of deformation processes and tensile tests were performed to observe the change of microstructure and the fracture behavior of this modified alloy. The observations of the microstructure and the cavities in tensile tests at elevated temperature have provided a better understanding of the deformation mechanism of AZ31–Zr–Sc alloy. The results indicate that both Sc and Zr precisely enhanced the grain refinement, and the proper process parameters also enhanced the ductility. The average grain size of the modified alloys was 3.5 μm after rolling and 2.03 μm after ECAE. The ductility of modified alloys after equal channel angular extrusion (ECAE) was 324% at 300 °C under tensile strain rate of 10^{-3} s^{-1}. Zr particles and fine nano-scale Mn–Sc precipitates were found in the microstructure. Based on the tensile test results, a PDA casing was successfully stamped with AZ31–0.15Zr–0.03Sc at 270 °C.

Keywords: Magnesium alloys; AZ31; Scandium; Zirconium; Mechanical properties; Grain size

1. Introduction

To develop a material process with both process productivity and material performance is necessary for development of a new alloy. The microstructures developed during hot deformation were studied for the sake of better formability and mechanical properties. The factors that affect the formability include suitable deformation parameters, deformation mechanisms of recovery and recrystallization, grain growth, and the characteristic of cavities.

The formability of AZ31 magnesium alloys was widely studied in the past decade [1–12]. There was inconsistency about the ductility of AZ31 at elevated temperature between different research results. Some researchers indicated that the ductility would remain increasing as the deformation temperature raised [13–15]. However, some researchers showed that there existed a peak value of elongation at the deformation temperature between 300 and 400 °C [16,17]. It is worth to study that whether there is an optimal temperature for hot deformation process. Meanwhile, all the studies above showed that the formability of AZ31 was strongly influenced by the grain size and morphology of the initial material microstructure, the process parameters (temperature, strain rate, deformation mechanism, etc.), the deformation mechanism, and the fracture mechanism. Also, it is well known that grain refinement may improve the ductility of magnesium alloys. However, hot deformation at elevated temperature still be affected by the thermal stability of these grain-refined magnesium alloys.

This paper proposed a new approach for development of grain-refined AZ31 alloy through adding minor Zr and Sc contents. Main objects were aimed at the effect on grain refinement and the tensile property. The examination was via observations of the microstructure and fracture mode by tensile test at elevated temperature. Stamping of a PDA casing was tested under the proper temperature derived from the tensile test to evaluate the performance of this modified AZ31–Zr–Sc alloy.

2. Experimental procedures

The modified AZ31–Zr–Sc magnesium alloys were prepared using commercial AZ31 and master alloys of Al–10Zr and Al–2Sc. The compositions of these alloys are listed in

* Corresponding author. Tel.: +886 3 5916997; fax: +886 3 5820207.
E-mail address: scwang@itri.org.tw (S.C. Wang).

0921-5093/$ – see front matter © 2007 Published by Elsevier B.V.
doi:10.1016/j.msea.2007.08.018

Table 1
Design alloy compositions used (wt.%)

Alloy type	Zr	Sc
AZ31	–	–
AZ31–0.15Zr	0.15	–
AZ31–0.15Zr–0.03Sc	0.15	0.03
AZ31–0.15Zr–0.06Sc	0.15	0.06

Table 1. The levels of Zr and Sc content were selected to determine the effects of these additions on grain refinement and hot formability. Casting was conducted at 700 °C under a protective gas of 0.03% SF_6. After casting, these materials were homogenized at 400 °C for 15 h and machined to 150 mm × 100 mm × 25 mm.

Rolling was conducted with a 2-Hi roller and the rolling temperature was 400 °C. Casting ingots were rolled in multi-passes to 3 mm, with a reduction ratio of 30% in each pass. Rolled specimens were then annealed at 300 °C for 30 min.

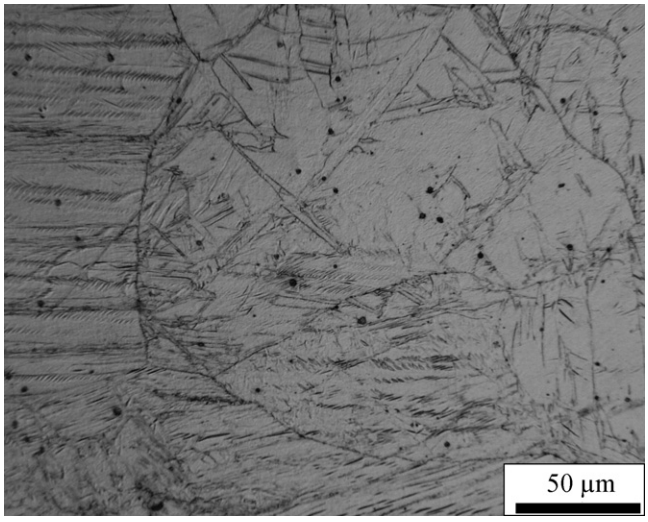

Fig. 1. Microstructure of the as-cast AZ31–0.05Zr–0.06Sc alloy.

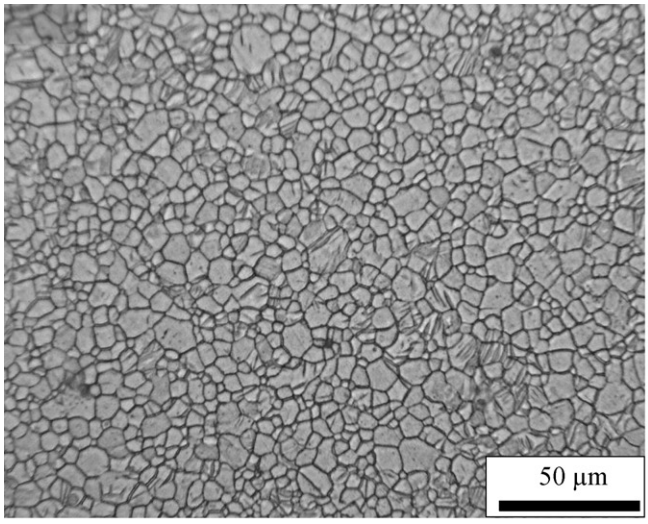

(a) AZ31

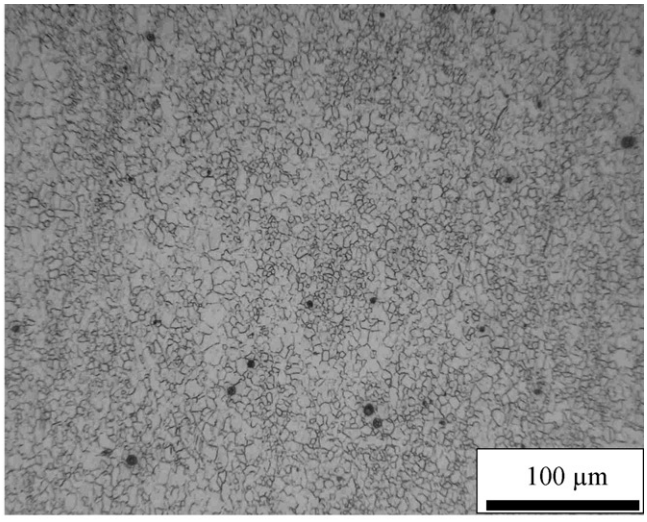

(b) AZ31-0.15Zr

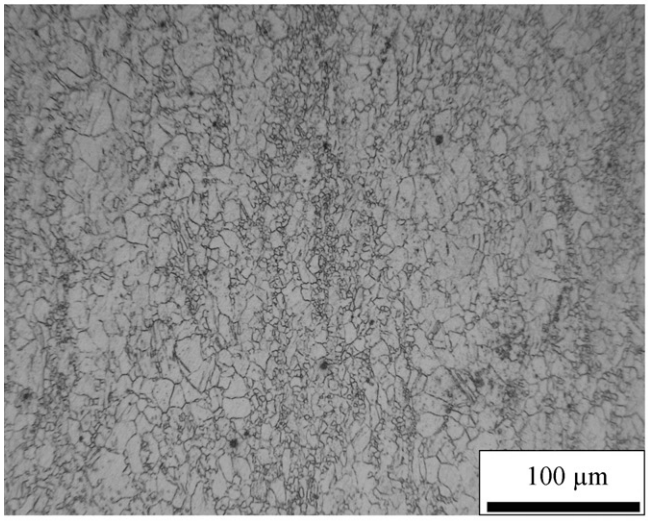

(c) AZ31-0.15Zr-0.03Sc

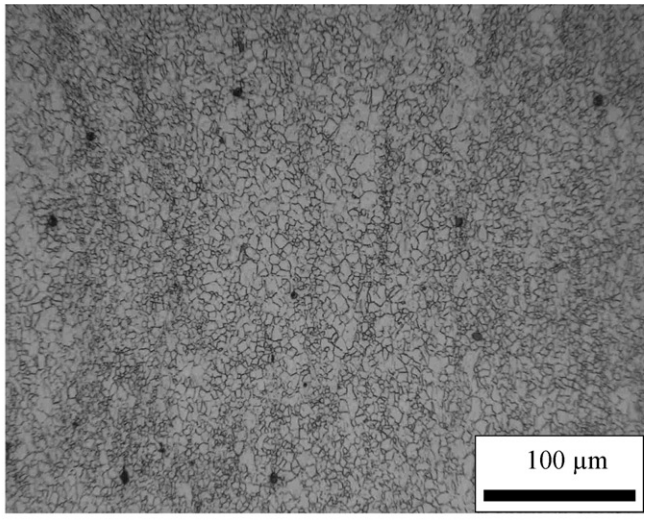

(d) AZ31-0.15Zr-0.06Sc

Fig. 2. Microstructures of the as-rolled specimen: (a) AZ31; (b) AZ31–15Zr; (c) AZ31–0.15Zr–0.03Sc; (d) AZ31–0.15Zr–0.06Sc.

Further ECAE test was employed to study the effect of pure shear deformation. Only the composition of AZ31–0.15Zr–0.03Sc was selected to compare the ductility with AZ31. The ECAE specimen size was 12 mm × 12 mm × 70 mm, the pressing temperature was 200 °C, the extrusion speed was 10 mm/s, and the internal angle Φ between two channels was 90°. The numbers of extrusion in ECAE were eight times. The ECAE test was conducted with a die fabricated by tool steel. The specimen was rotated by 90° about the longitudinal axis and reloaded from another end between consecutive passes. The specimens after ECAE were annealed at 190 °C for 1 h.

Tensile tests were performed on Instron with a temperature-controlled furnace to maintain the specimens test at the elected temperature. The temperature difference of the specimens was controlled within ±3 °C. The strain rate was 10^{-3} s^{-1}.

The rolled only, ECAE tested, and tensile tested specimens were sectioned along the deformation direction to measure the grain size and examine the microstructure by optical microscopy. The linear intercept method was used to measure the average

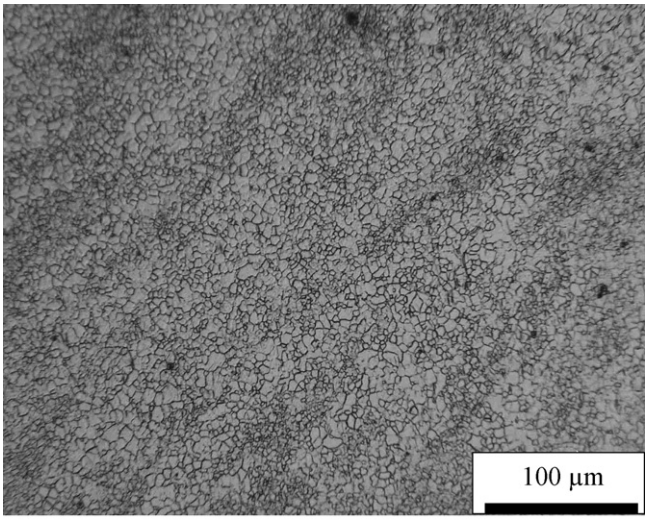

(a) AZ31-0.15Zr-0.03Sc

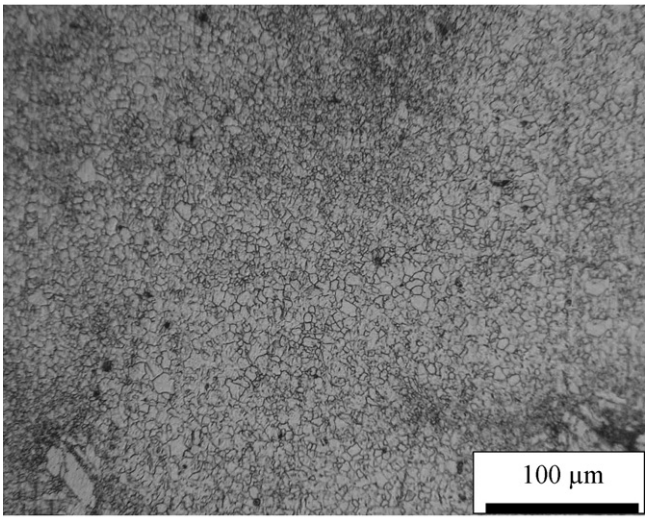

(b) AZ31

Fig. 3. The microstructures after ECAE: (a) AZ31–0.15Zr–0.03Sc; (b) AZ31.

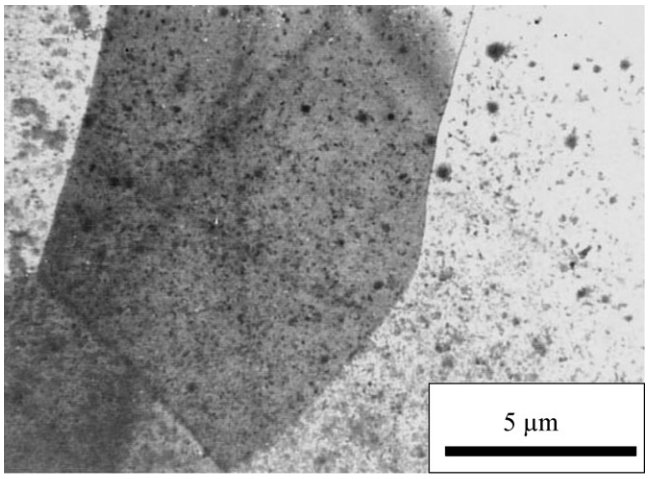

(a) Fine precipitates of Mn and Zr dispersed uniformly in AZ31-0.15Zr-0.03Sc

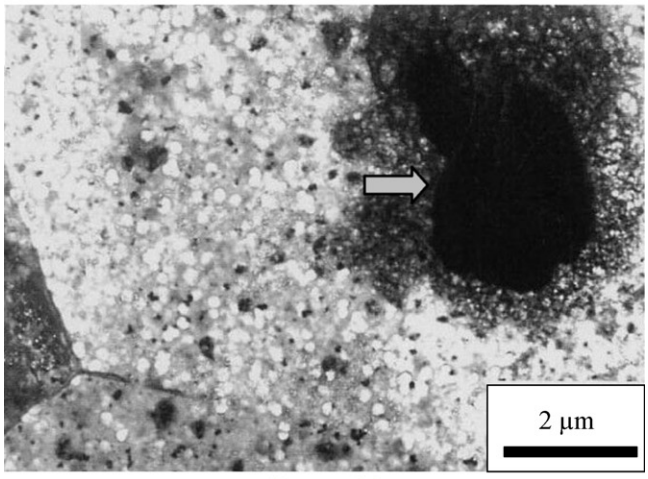

(b) Zr particle

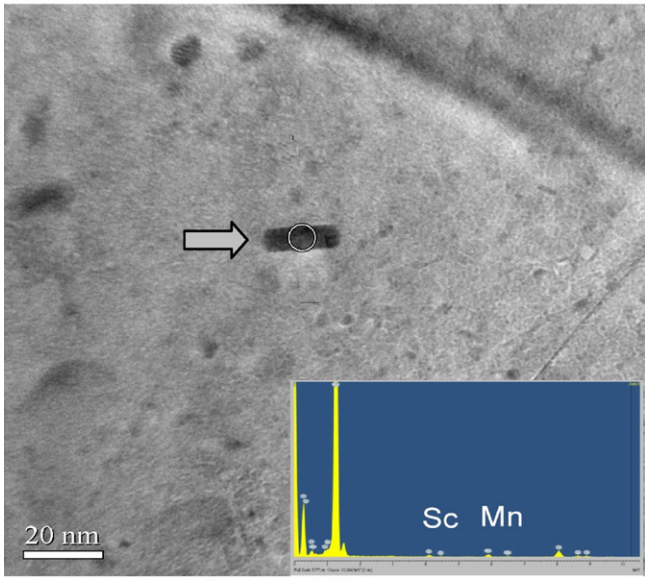

(c) Nano-scale Mn-Sc precipitates

Fig. 4. Precipitates of AZ31–0.15Zr–0.03Sc: (a) fine precipitates dispersed uniformly after rolled and annealed at 300 °C for 1 h; (b) Zr particle; (c) nano-scale Mn–Sc precipitates.

grain size. Also, special attention was given to the morphology of the grain distribution and fracture surface after deformation processes. TEM was performed to identify further detail characters of the microstructures.

The stamping tests of PDA casing were performed with the ECAE AZ31–0.15Zr–0.03Sc and AZ31 materials. The initial thickness was 1.2 mm. The stamping specimens were heating to 270 or 350 °C for 10 min, and the die temperature was held at 160 °C. A hydraulic pressing machine was used to perform the stamping tests. Observation was focus on the fracture of crack and the surface condition.

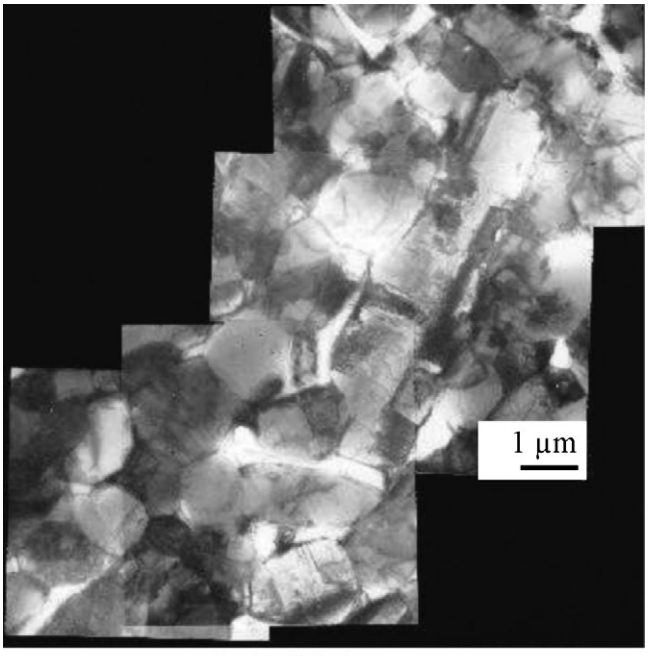

(a) As-rolled microstructure

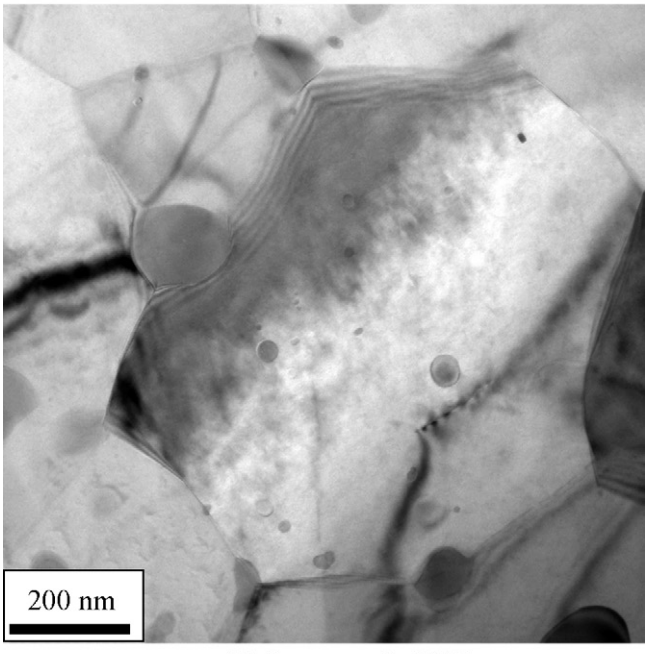

(b) Microstructure after ECAE

Fig. 5. The TEM microstructure of AZ31–0.15Zr–0.03Sc at: (a) as-rolled; (b) after ECAE.

3. Results and discussion

The microstructure of AZ31–0.15Zr–0.06Sc is identical to typical as-casted AZ31 as shown in Fig. 1. The grain size range is between 50 and 200 μm. It can be noticed that the addition of Zr and Sc and the their content level did not affect the grain size in the as-casted sample. But after rolling, it makes a big difference. The microstructures of as-rolled specimens are shown in Fig. 2. The average grain size of the modified alloys (3.5 μm) is much smaller than that of AZ31 alloy (7.5 μm). The grain size can be even more refined by ECAE treatment. As shown in Fig. 3, the average grain sizes are 2.03 and 2.99 μm for AZ31–0.15Zr–0.06Sc and AZ31, respectively. The function of Zr and Sc, forming invisible nano-precipitates in the matrix phase [16], can be clearly observed through the fine grain and uniform microstructure of mechanically deformed AZ31–0.15Zr–0.06Sc alloys. While in the AZ31 alloy, some

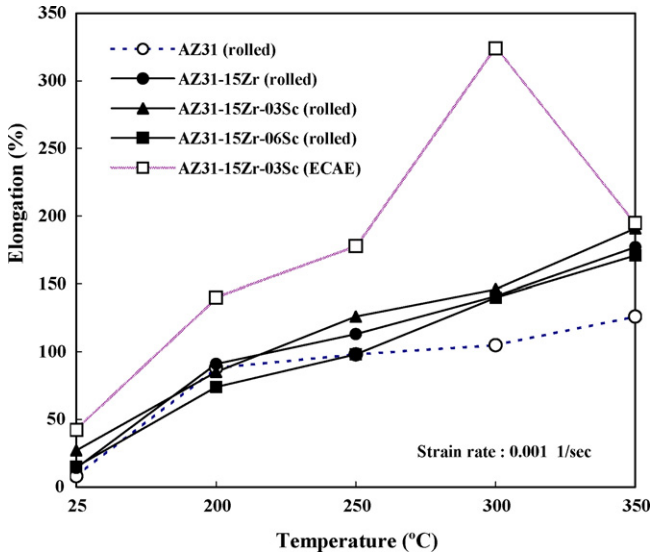

Fig. 6. The ductility of modified AZ31–Zr–Sc alloys and AZ31 at elevated temperature.

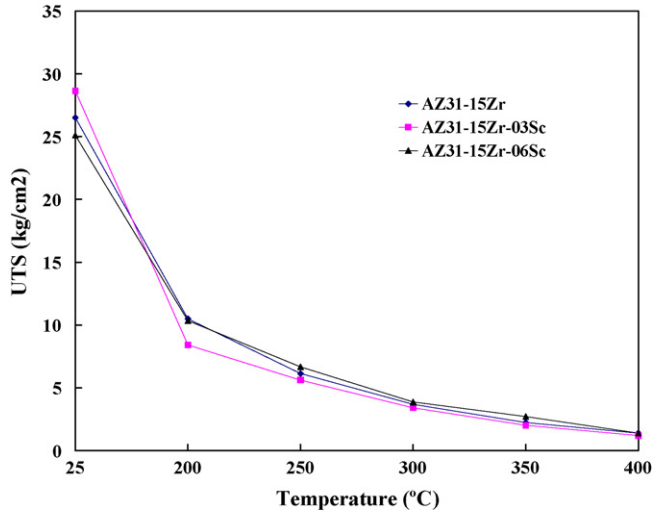

Fig. 7. The strength of rolled AZ31–Zr–Sc alloys at elevated temperature.

large grains can be easily identified even though it had been applied the same mechanical deformation.

TEM microphotographs of AZ31–0.15Zr–0.03Sc alloy were taken after being annealed at 300 °C for 30 min. Fig. 4 presents many Zr, Sc and Mn precipitates in the matrix phase of Mg. The microstructures are comprised mostly an Mg-rich phase, precipitates of $Al_{12}Mg_{17}$, and some randomly dispersed Mn particles (Fig. 4(a)) and Zr-rich particles (Fig. 4(b)). There were many fine precipitates uniformly distributed in the rolled materials. As shown in Fig. 4(c), those particles (20 nm) are Mn–Sc precipitates. The grain boundaries were pinned immobile after rolling or after ECAE processing, thereof. While in AZ31, there were no fine particles to restrict the grain boundary migration after rolling when the samples were still left at high temperature. In order to identify the content of those particles, the sample was annealed at 400 °C for 15 min for particle growth. It is well known that

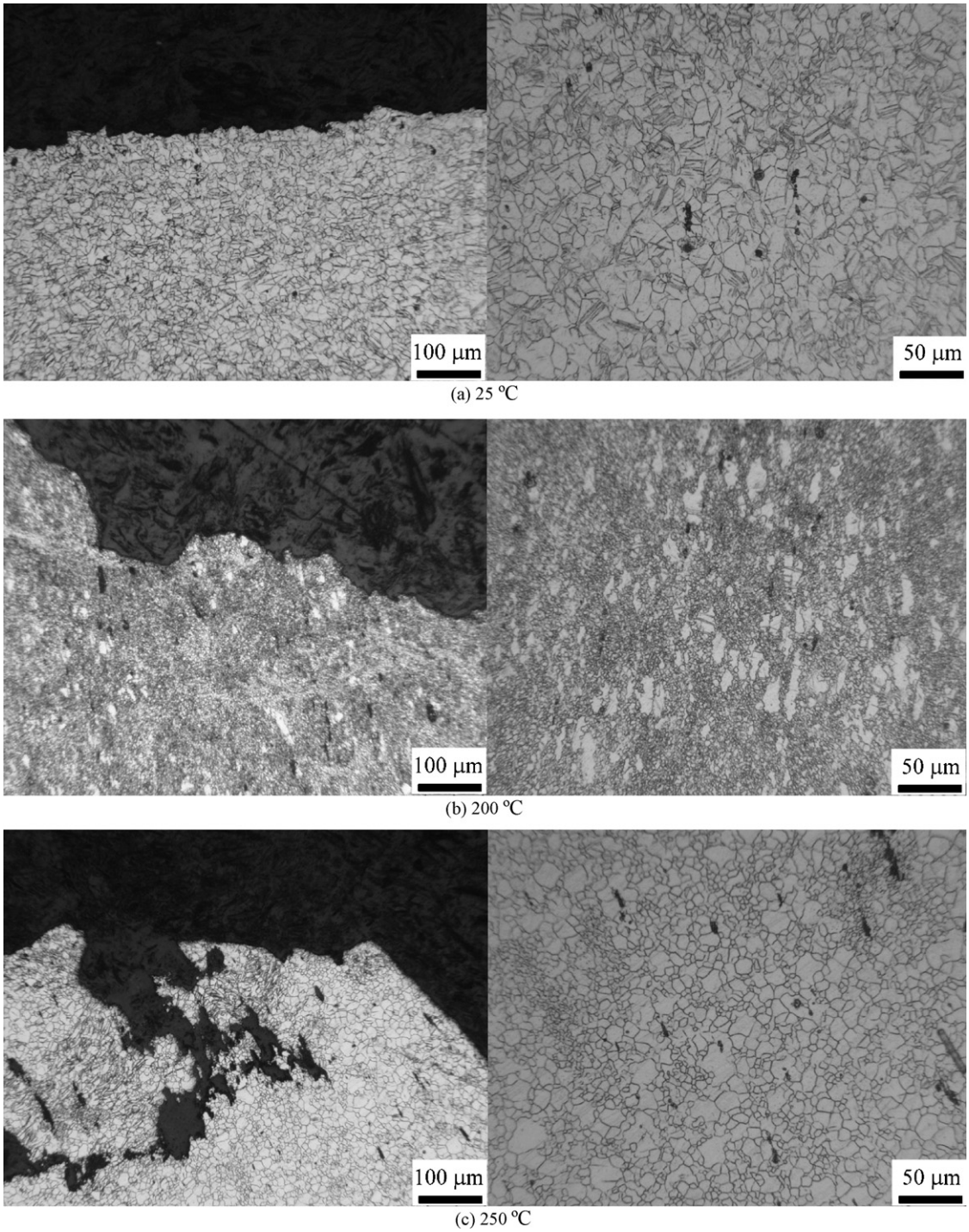

Fig. 8. The cavities at and near the tensile fracture surface of rolled AZ31–0.15Zr–0.03Sc tested at: (a) 25 °C; (b) 200 °C; (c) 250 °C; (d) 300 °C; (e) 350 °C; (f) 400 °C.

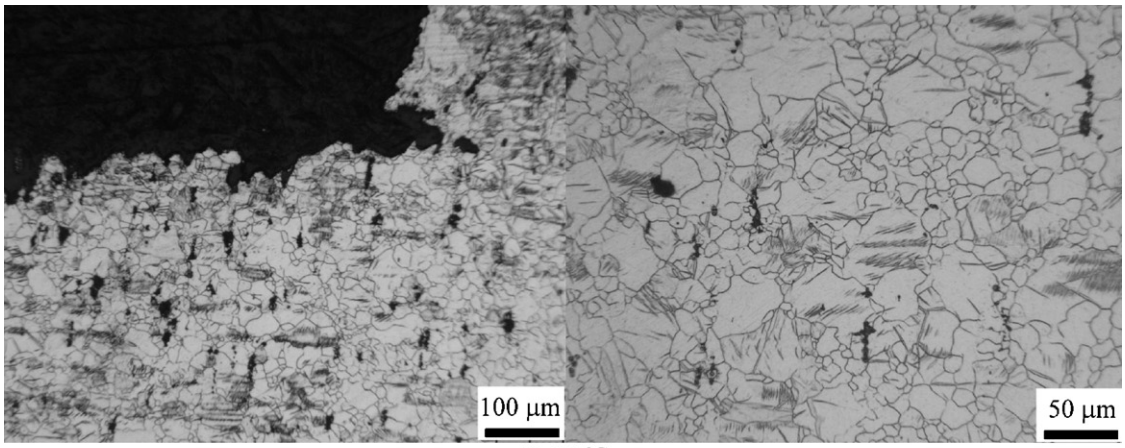

(d) 300 °C

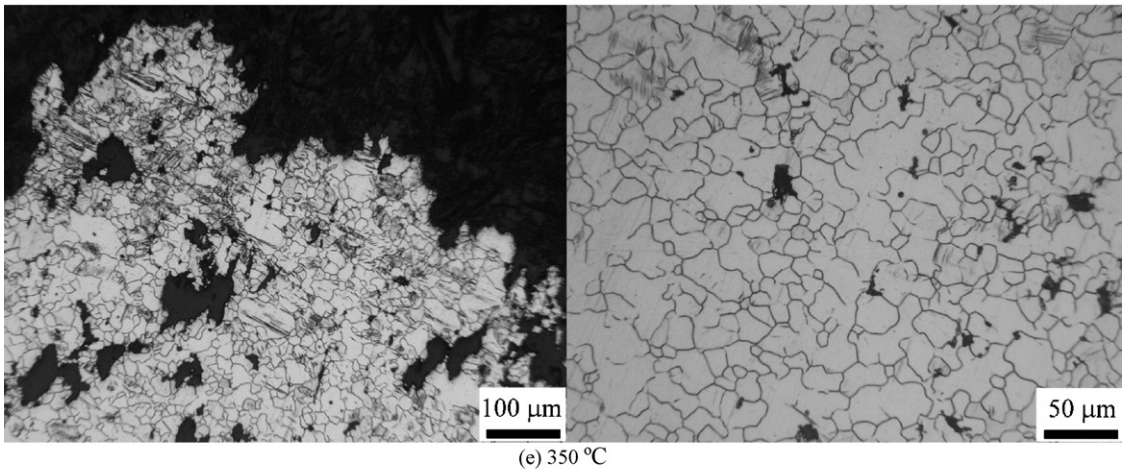

(e) 350 °C

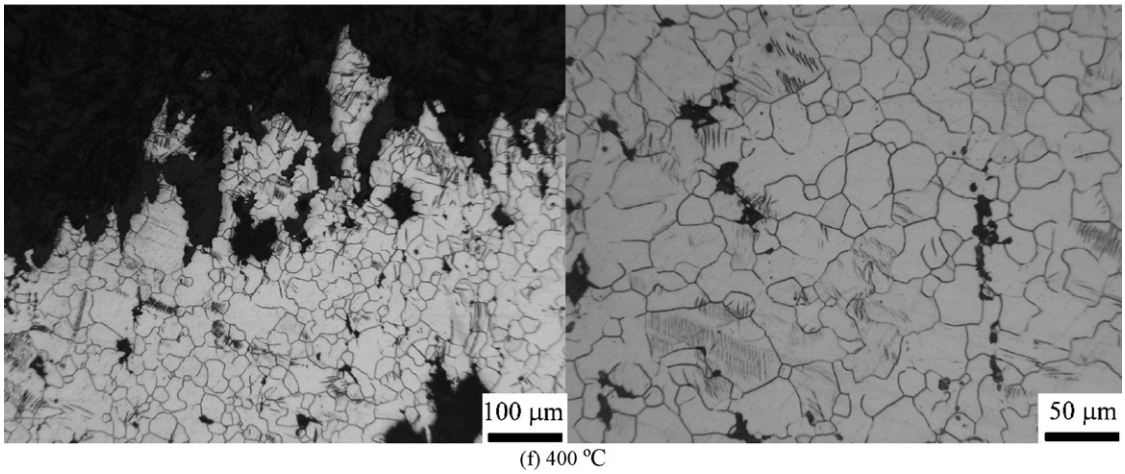

(f) 400 °C

Fig. 8. (*Continued*).

small particle (<0.4 μm) may retard continuous recrystallization by pinning sub-grain boundaries and preventing sub-grain coalescence [18]. This is in good agreement with what has been observed function of Mn–Sc precipitates in AZ31–Zr–Sc system. Through TEM observation, there were some differences between rolled and ECAE samples around grain boundary region can be identified (Fig. 5). In Fig. 5(a), there were plenty of dislocations near the grain boundaries of the rolled specimens. While in ECAE samples (Fig. 5(b)), there were fewer dislocations but many small grains near the grain boundaries of large grains. Although these phenomena need more investigation, it apparently indicates that the ECAE process may provide a more stable material for hot working.

The tensile test results are presented in Fig. 6. The elongation of all specimens increased with the increase of the testing temperatures, except for the ECAE specimen tested at 350 °C. As temperatures were at or lower than 250 °C, the elongation behaviors of AZ31–Zr–Sc and AZ31 were almost the same. But when

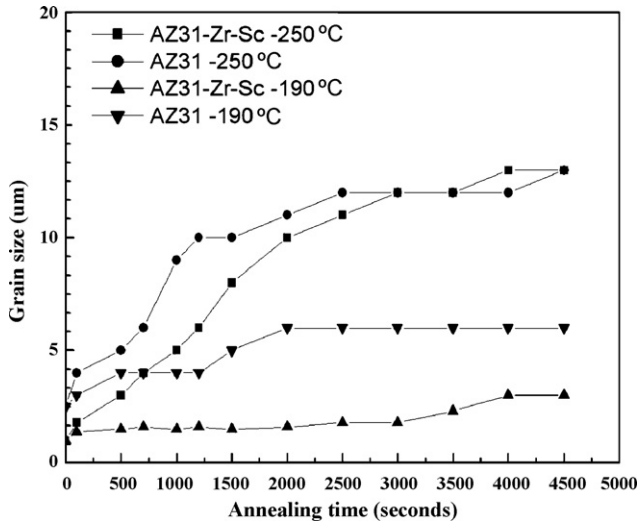

Fig. 9. The grain growth of AZ31 and AZ31–0.15Zr–0.03Sc that after ECAE and annealed at 190 and 250 °C.

the temperatures exceeded 250 °C, the difference was emerged and the elongation of AZ31–Zr–Sc was greater than AZ31 for 25–50%. The data of the strength of the rolled alloys were shown in Fig. 7. As the test temperature raised, the strength decreased with a linear slope. There was no difference between different alloys.

The deformation mechanism was mainly the deformation twinning at room temperature (Fig. 8(a)). The cavities can be observed in the deformed microstructure. When the test temperature raised to 200 °C, there were a lot of large grains in the tensile direction and surrounded by fine recrystallized grains, as shown in Fig. 8(b). The deformation mechanism had been changed from deformation twinning to dynamic recrystallization. It is well known that dynamic recrystallization will be nucleated at the twin area [19]. Our observation revealed that the microstructure had been transformed from deformation twins (room temperature) to recrystallized grains (200 °C). When the temperature raised from 250 to 300 °C, uniformly grain growth were observed. The cavity number was about the same but the cavity size became larger. The microstructure showed that the dynamic recrystallization continuous developed, as can be seen in Fig. 8(c and d). No elongated grain was observed, several cavities were developed between the equaixed grains and formed a serrated surface at the fracture tip. As the temperature increased from 350 to 400 °C, the deformation mechanism was changed to grain coalescence and grain deformation. The cavities began to link up together (Fig. 8(e and f)). Lee and Huang [20] had studied the cavitation characteristics of AZ31 during deformation at elevated temperature. The cavity nucleation only occurred at the very early stage and cavity growth dominated most of the straining process. Through observation, our results have the same conclusion, i.e. the cavities dominated

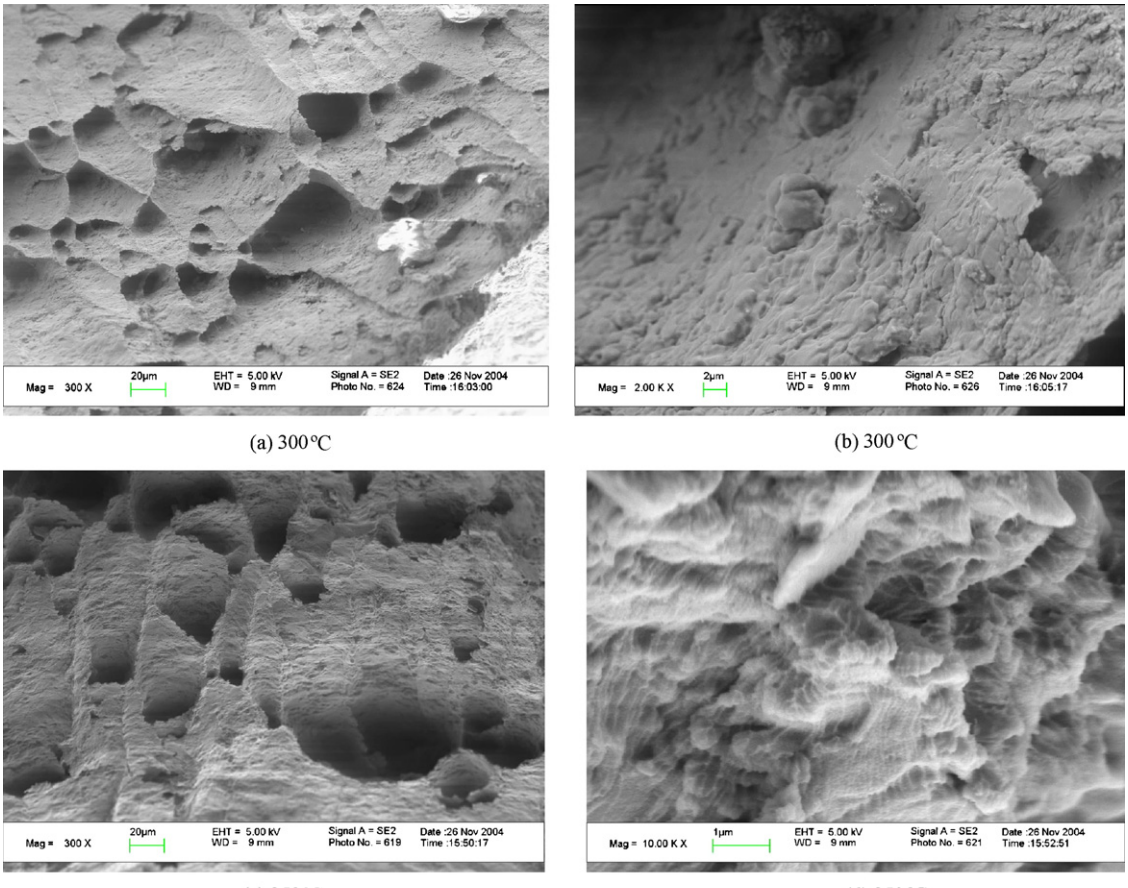

(a) 300 °C (b) 300 °C

(c) 350 °C (d) 350 °C

Fig. 10. The SEM of the fracture surface of AZ31–0.15Zr–0.03Sc after ECAE tested at; (a and b) 300 °C; (c and d) 350 °C.

the results of tensile deformation. According to the microstructure of the tensile test results, we concluded that the deformation mechanism has been changed through following stages: deformation twinning, dynamic recrystallization, grain coalescence and grain deformation. The cavity growth dominated the fracture and was controlled by superplasticity diffusion (Nabarro-Herring phenomena) when the test temperature exceeded 250 °C.

The resistance of grain growth at elevated temperature will be a mainly concern during following hot deformation process. In order to understand the grain growth at elevated temperature, further annealing tests of AZ31–0.15Zr–0.03Sc and AZ31 were performed (Fig. 8). When the heating temperature was at 190 °C, the grain size of AZ31–Zr–Sc remains unchanged, while the grain size began to grow for AZ31. When the heating temperature was at 250 °C, the grain of these two alloys both began to grow. The grain growth rate of AZ31–0.15Zr–0.03Sc was smaller than that of AZ31 as shown in Fig. 9. The grain grows apparently as the annealing time increase. These two alloys had the same grain size after heating for 50 min at 250 °C. It is noticed that the heating time was only 10 min in the tensile test, the grain size of the modified alloys might be smaller than the grain size of AZ31 at the same heating conditions (Fig. 10).

Fig. 6 presents the elongation of rolling and ECAE specimens. The ductility of ECAE specimens exceeded that of the rolled specimens obviously. The ductility of the rolled specimen was 14–27% at room temperature, while that of ECAE specimen was 42% at room temperature. As the temperature increased, the difference of ductility increased. The maximum difference happened at 300 °C. The ductility of the rolled specimen was 140% at 300 °C, while that of ECAE specimen was 324% at 300 °C. The slow grain growth rate of the modified alloy was why the ductility of modified alloys was better than AZ31in the tensile tests. The ductility of the modified alloy after ECAE was dropped at temperature higher than 300 °C. This phenomenon was the same with the results of some prior studies [16,17,21], the ductility may be decreased due to some precipitates solute into matrix and the grain growth become faster as the teat temperature reach a critical point. To find the reason that responsible for this, SEM was performed to examine the fracture surfaces. When the test temperature was at 350 °C, the cavities began to grow and cross-link to each other (Fig. 9(c)). Under a higher magnification (Fig. 9(d)), the fracture surface revealed many step marks, instead of pure shear slip lips that developed in 300 °C (Fig. 9(b)). The material seemed to lose the strength and ductility suddenly at such a high temperature.

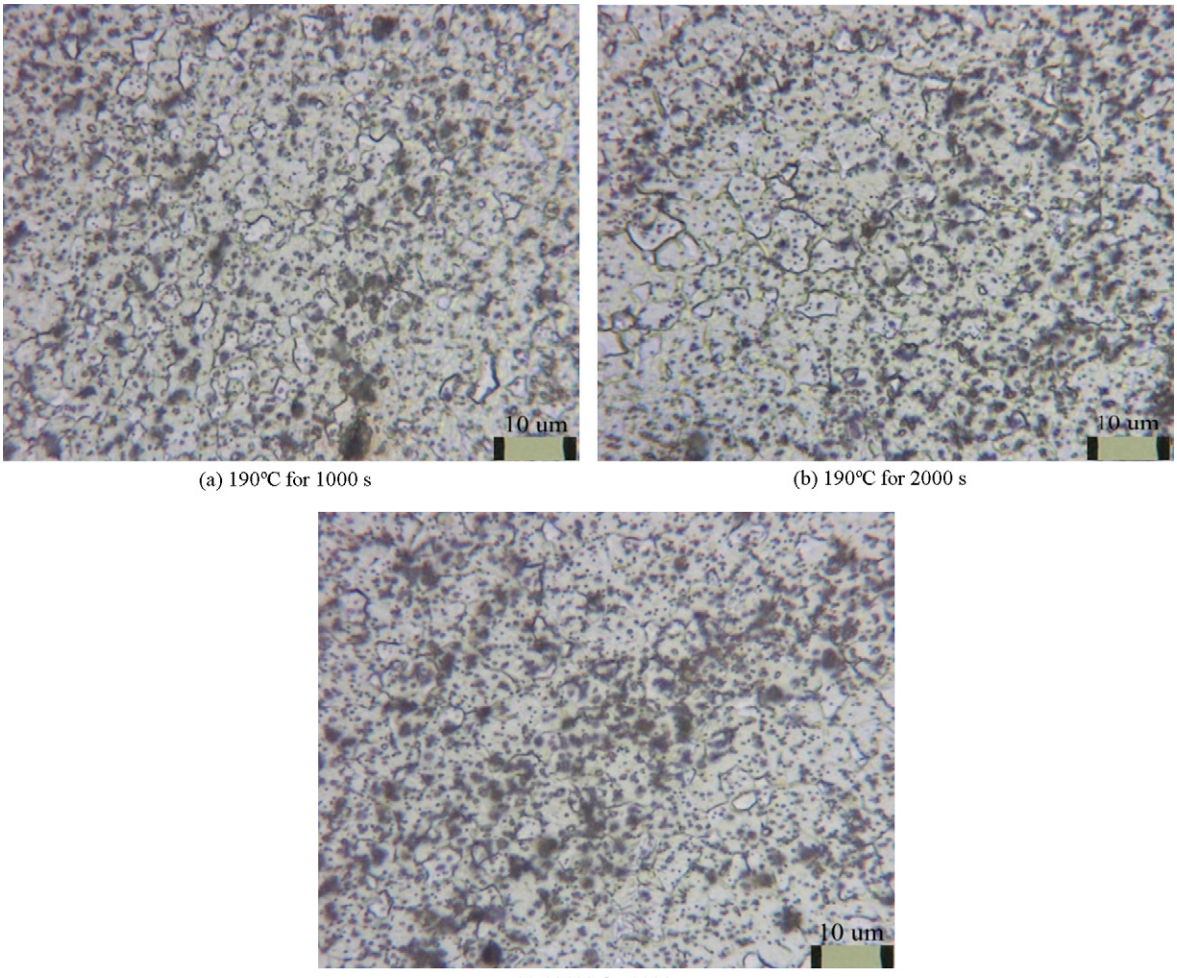

(a) 190℃ for 1000 s

(b) 190℃ for 2000 s

(c) 190℃ for 3000 s

Fig. 11. Microstructure of modified AZ31–0.15Zr–0.03Sc annealed at 190 °C for: (a) 1000 s; (b) 2000 s; (c) 3000 s.

del Valle et al. [22] had pointed out that there are two individual deformation mechanisms of magnesium alloys at high temperature deformation, i.e. GBS and crystallographic slip (CS). GBS, accommodated by grain-boundary diffusion, seem to play an important role during deformation in the low-strain-rate range. The CS would take over as grain growth occurs. Tan et al. [14] indicated that the large grain is not suitable for GBS. Only grains with an average grain size of smaller than 10 μm and possess high misorientation angles can be deformed by GBS. Since the ECAE specimens had smaller grain size than the rolled specimens, it is reasonable that the ductility of ECAE specimens were better than that of rolled specimens

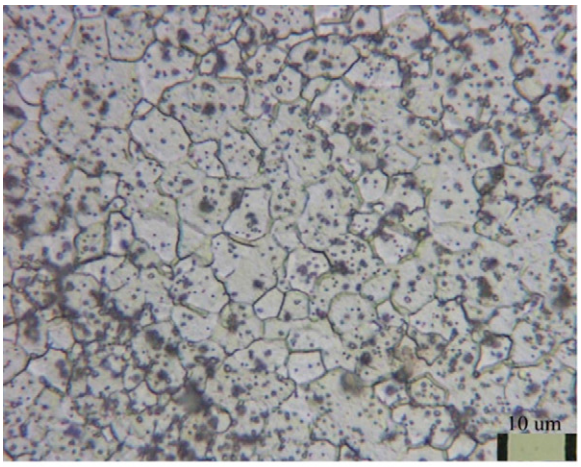

(a) 250°C for 1000 s

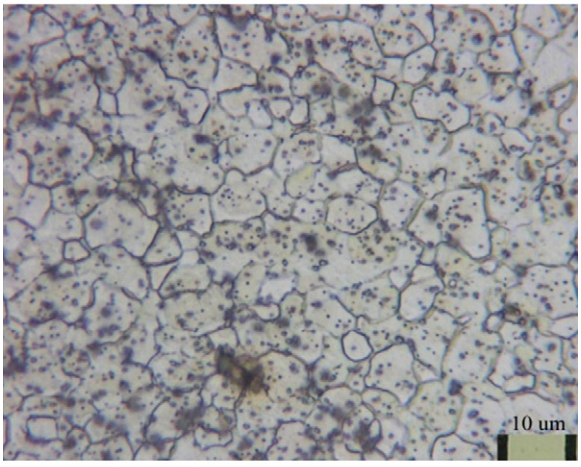

(b) 250°C for 2000 s

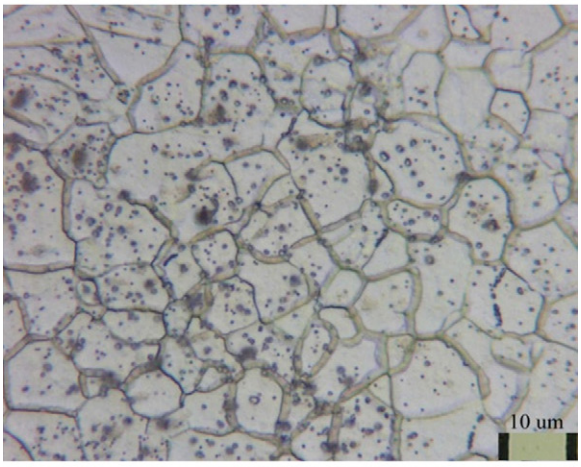

(c) 250°C for 3000 s

Fig. 12. Microstructure of modified AZ31–0.15Zr–0.03Sc annealed at 250 °C for: (a) 1000 s; (b) 2000 s; (c) 3000 s.

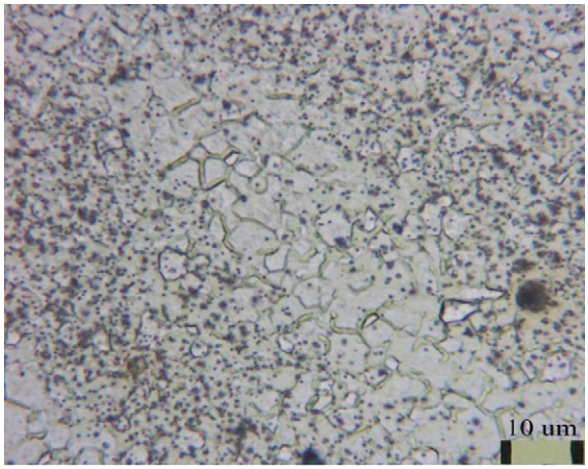

(a) 190°C for 1000 s

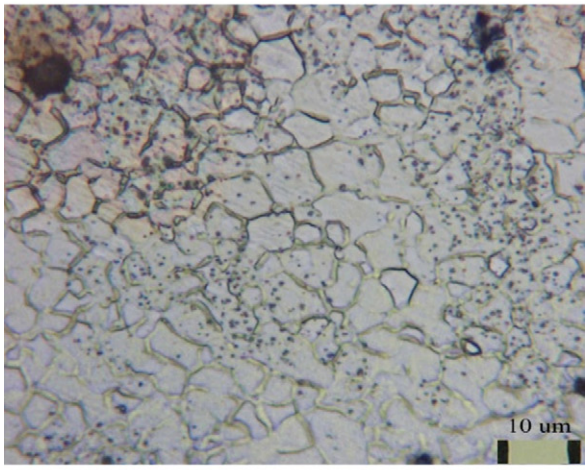

(b) 190°C for 2000 s

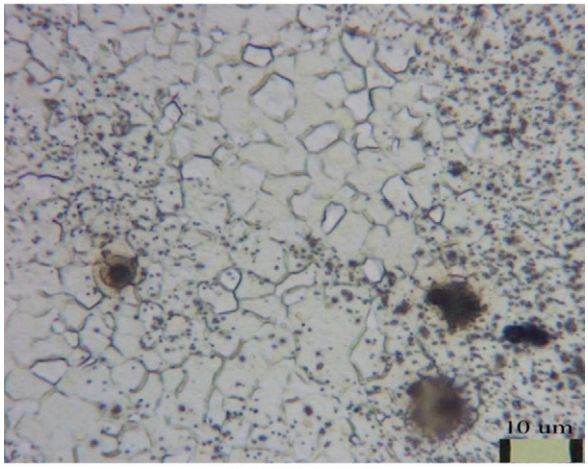

(c) 190°C for 3000 s

Fig. 13. Microstructure of modified AZ31 annealed at 190 °C for: (a) 1000 s; (b) 2000 s; (c) 3000 s.

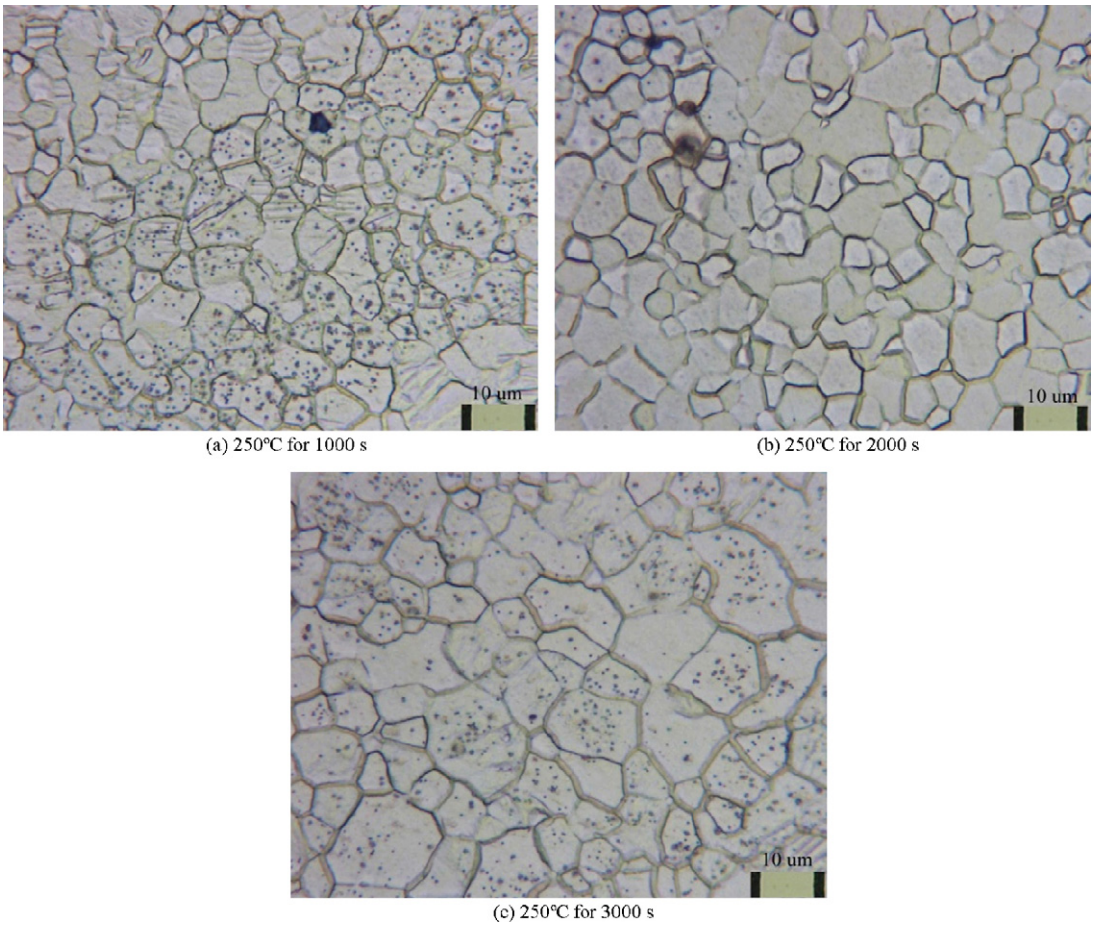

(a) 250℃ for 1000 s (b) 250℃ for 2000 s

(c) 250℃ for 3000 s

Fig. 14. Microstructure of modified AZ31 annealed at 250 °C for: (a) 1000 s; (b) 2000 s; (c) 3000 s.

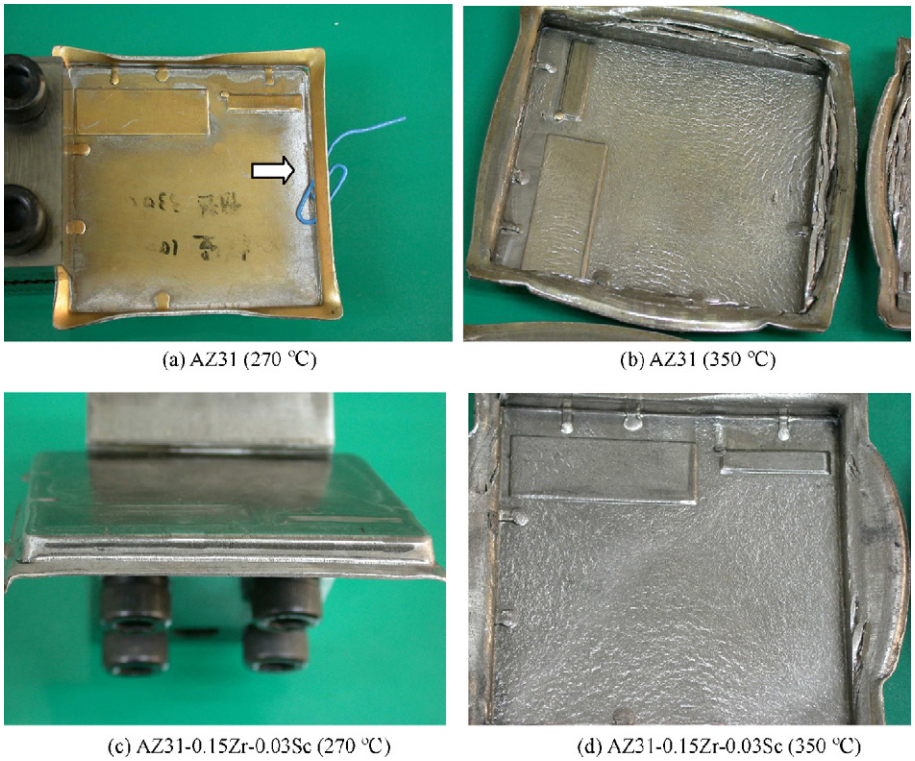

(a) AZ31 (270 ℃) (b) AZ31 (350 ℃)

(c) AZ31-0.15Zr-0.03Sc (270 ℃) (d) AZ31-0.15Zr-0.03Sc (350 ℃)

Fig. 15. Pictures of stamping of a PDA casing: (a) AZ31 (270 °C); (b) AZ31 (350 °C); (c) AZ31–0.15Zr–0.03Sc (270 °C); (d) AZ31–0.15Zr–0.03Sc (350 °C).

at temperature below 300 °C. From Fig. 7(d and e), it is noticed that the grain size near the fracture tip grew rapidly as temperature raised form 300–350 °C. The grains near the fracture tip had grew rapidly to over 10 μm, a lot of grains near the fracture tip even grew up to 50 μm. The deformation mechanism of the ECAE specimens might have been changed from GBS to CS with such large grain at 350 °C. The ductility soon dropped down to the same level of the rolled specimens. Those fine step marks in Fig. 9(d) might be the evidence that the deformation mechanism had changed from GBS to slip deformation as the temperature raised to 350 °C. The results may be explained why the ductility of ECAE specimen suddenly dropped at 350 °C.

Further examining the microstructures reveals the grain growth curve during annealing. This main factor that influenced the grain growth may be the precipitates in the microstructure, as presented in Figs. 11–14. The amounts of precipitates in AZ31–0.15Zr–0.03Sc (Figs. 11 and 12) were more than those in AZ31 (Figs. 13 and 14). The precipitates in AZ31–0.15Zr–0.03Sc were numerous and distributed uniformly, while those in AZ31 dissolved into the matrix as the heating time increased. This observation reveals that the fine precipitates of the modified AZ31–Zr–Sc alloy were very important in affecting the grain growth during annealing.

The stamping of the PDA casing was performed with ECAE materials. Because the heating time was only 10 min, according to the grain growth rate derived from Fig. 8, the grain size of the specimens were remain below 10 μm. The results of stamping tests were shown in Fig. 14. The stamping of AZ31 alloy reveals many small cracks at the edge and at the surface of the casing, both at 270 °C (Fig. 14(a)) and 300 °C (Fig. 14(b)). However, the stamping of modified AZ31–0.15Zr–0.03Sc alloy was without crack at 270 °C (Fig. 14(c)), but failed at 350 °C (Fig. 14(d)). The results of stamping test were complete confirmed with the results of tensile test, i.e. ductility would dropped suddenly when the temperature was over 300 °C. The modified AZ31–Zr–Sc alloys were suitable for hot deformation under special process conditions. An advanced study on the processing window of the forming parameters is needed for a stable product processes (Fig. 15).

4. Summary

This paper has presented the effects on the microstructure and mechanical properties of AZ31 by adding Zr and Sc. The grain size and the ductility of modified AZ31–Zr–Sc alloys were both enhanced. The average grain size of the modified alloys was 3.5 μm after rolling and 2.03 μm after ECAE. The ductility of modified alloys after ECAE was 324% at 300 °C.

Better resistance to grain growth at elevated temperature was achieved, the grain size of AZ31–0.15Zr–0.03Sc was still under 3 μm by heating at 190 °C for 1 h and under 10 μm by heating at 250 °C for 30 min.

Fine Zr particles and nano-scale Mn–Sc precipitates were found in the modified alloy. The superior grain refinement and ductility may be caused by the dispersion of these fine precipitates. The further understanding of these fine precipitates on grain refinement and enhancement of ductility are still under further study.

The results of stamping test were succeeded and excited. This means that the productions for 3C casing may be predominated by processing of this modified alloy. This could be a very important achievement for the magnesium industry.

Acknowledgements

The authors are grateful to C.S. Chen, PhD, C.M. Chen and Y.C. Fann for assistance with experiments. Thanks to A.K. Li, PhD and C.C. Yang, PhD of Industrial Technology Research Institute for helpful suggestions.

References

[1] A. Yamashita, D. Yamaguchi, Z. Hortia, T.G. Langdon, Mater. Sci. Eng. A287 (2000) 100–106.
[2] A. Yamashita, Z. Hortia, T.G. Langdon, Mater. Sci. Eng. A300 (2001) 142–147.
[3] A. Bussiba, A. Ben Artzy, A. Shtechman, S. Ifergan, M. Kupiec, Mater. Sci. Eng. A302 (2001) 56–62.
[4] W.J. Kim, C.W. An, Y.S. Kim, S.I. Hong, Scripta Mater. 47 (2002) 39–44.
[5] T.C. Chang, J.Y. Wang, C.M. O, S. Lee, J. Mater. Process. Technol. 140 (2003) 588–591.
[6] K. Matsubara, Y. Miyahara, Z. Horita, T.G. Langdon, Acta Mater. 51 (2003) 3073–3084.
[7] C.W. Su, B.W. Chua, L. Lu, M.O. Lai, Mater. Sci. Eng. A402 (2005) 163–169.
[8] L. Jin, D. Lin, D. Mao, X. Zeng, W. Ding, Mater. Lett. 59 (2005) 2267–2270.
[9] Y. Miyahara, K. Matsubara, Z. Horita, T. Langdon, Metall. Mater. Trans. 36A (2005) 1705–1711.
[10] J.Y. Wng, Y.H. Chen, Y.L. Yang, S. Lee, Mater. Sci. Forum 488/489 (2005) 465–472.
[11] L. Yang, X.M. Yang, T. Liu, S.D. Wu, L.J. Chen, Mater. Sci. Forum 488/489 (2005) 575–580.
[12] L. Lin, L. Chen, Z. Kiu, Mater. Sci. Forum 488/489 (2005) 581–584.
[13] E. Krajewski, in: H.I. Kaplan (Ed.), Proceedings of Magnesium Technology 2002, TMS, Seattle, 2002, pp. 175–197.
[14] J.C. Tan, M.J. Tan, Mater. Sci. Eng. A339 (2003) 124–132.
[15] D.L. Yin, K.F. Zhang, G.F. Wang, W.B. Han, Mater. Lett. 59 (2005) 1714–1718.
[16] A. Mwembela, E.B. Konopleva, H.J. McQueen, Scripta Mater. 37 (1997) 1789–1795.
[17] F.K. Chen, T.Y. Huang, J. Mater. Process. Technol. 142 (2003) 643–647.
[18] J.C. Williams, E.A. Starke Jr., in: G. Krauss (Ed.), Deformation, Processing, and Structure, 1982, pp. 285–286.
[19] M.M. Myshlyaev, H.J. McQuen, A. Mwembela, E. Konopleva, Mater. Sci. Eng. A337 (2002) 121–133.
[20] C.J. Lee, J.C. Huang, Acta Mater. 52 (2004) 3111–3122.
[21] V.N. Chuvil'deev, T.G. Nieh, M.Y. Gryaznov, A.N. Sysoev, V.I. Kopylov, Acta Mater. 50 (2004) 861–865.
[22] J.A. del Valle, M.T. Pérez-Prado, O.A. Ruano, Metall. Mater. Trans. 36A (2005) 1427–1438.